Available online at www.sciencedirect.com
ScienceDirect
Journal of Luminescence 125 (2007) 55–59
JOURNAL OF LUMINESCENCE
www.elsevier.com/locate/jlumin

Phonon physics in ruby studied by optical pumping and luminescence

H.W. de Wijn*

Department of Physics and Astronomy, and Debye Institute, Utrecht University, P.O. Box 80000, 3508 TA Utrecht, The Netherlands

Available online 12 September 2006

Abstract

Two examples are treated of nonequilibrium phonons in ruby as studied with optical pumping for generation and luminescence for detection. The first example concerns nonequilibrium 29 cm^{-1} and near-zone-boundary phonons generated in the nonradiative decay from higher multiplets to $2\overline{A}(^2E)$ and $\overline{E}(^2E)$. The second example shows that coherent phonons are produced by stimulated emission over the Zeeman transition within the $\overline{E}(^2E)$ metastable doublet.

Keywords: Spin-lattice relaxation; Non-equilibrium phonons; Coherent phonons; Stimulated emission

1. Introduction

This *Festschrift* article is written in honor of Alexander Kaplyanskii on the occasion of his 75th birthday. Professor Kaplyanskii played a decisive role in, among other fields, the physics of phonons. The aims of the article are to introduce the reader to the use of luminescent centers for the generation and detection of phonons, and to show what ruby (dilute Cr^{3+} in Al_2O_3) in particular has contributed to phonon physics. This is demonstrated with the help of two examples, which may serve as ''opening and closing brackets'' of over three decades of phonon research by optical pumping and luminescence. The first one is a remarkable riddle dating from the early days of optical phonon research, which was solved by the Kaplyanskii group. The second example concerns coherence of phonons emitted by stimulated emission.

2. Generation and detection

For the generation and detection of phonons by optical methods one generally makes use of a one-phonon transition connecting two closely lying luminescent states. To detect phonons, the *lower* of the two states is populated, and any population of the upper state as a result of absorption of phonons is observed via the luminescence emanating from this state [1]. Note that this scheme has an inherent energy amplification in that, in principle, a phonon releases an optical photon. The luminescent states may conversely be used for the generation of phonons by populating the *upper* state to sufficient density, and letting it decay over the one-phonon transition.

In ruby, a one-phonon transition is present between the $\overline{E}(^2E)$ and $2\overline{A}(^2E)$ Kramers doublets of Cr^{3+}, which is subject to a tetragonally distorted cubic crystalline field. As depicted in Fig. 1, the $2\overline{A}(^2E)$ doublet is at a distance of 29 cm^{-1} above $\overline{E}(^2E)$. The latter is at 14.430 cm^{-1} above the $^4A_2$ ground multiplet, to which it returns via the R_1 luminescence with a radiative lifetime $\tau_R \sim 4$ ms. The degeneracy of the doublets and the 29 cm^{-1} phonon transition may be removed by an external magnetic field, as is in fact done in Section 3. Another interesting one-phonon transition in the ruby system is the one connecting the two $\overline{E}(^2E)$ states split in a field, because, as discussed in Section 4, it is sufficiently narrow to allow the generation of coherent phonons.

3. Near-zone-boundary and 29-cm^{-1} phonons

In 1969, Geschwind, Walker, and I performed a number of investigations by optical pumping and luminescence in an attempt to quantify the dynamics of nonequilibrium 29-cm^{-1} phonons in ruby. The Orbach relaxation in $\overline{E}(^2E)$ due to these phonons had shortly before been studied in detail by Geschwind et al. [2].

*Tel.: +31 30 2532227; fax: +31 30 2532403.
E-mail address: h.w.dewijn@phys.uu.nl.

0022-2313/$ - see front matter © 2006 Elsevier B.V. All rights reserved.
doi:10.1016/j.jlumin.2006.08.024

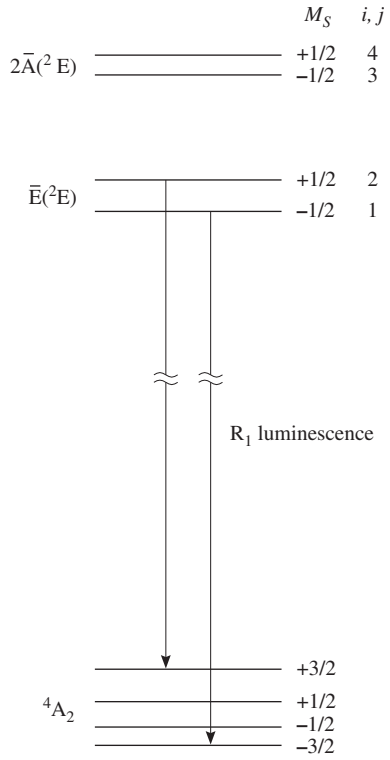

Fig. 1. The level scheme of Cr^{3+} in dilute ruby in a magnetic field along the c axis. The $\overline{E}(^2E)$ and $2\overline{A}(^2E)$ Kramers doublets are at a distance of $29\,cm^{-1}$, and $\overline{E}(^2E)$ is situated at $14.430\,cm^{-1}$ above the $^4A_2$ ground quartet.

The ruby specimens were small single crystals, approximately $1\times1\times5\,mm^3$ in size. They contained Cr^{3+} substitutionally at the Al sites at the quite dilute concentrations of 40 and 340 at.ppm, among other things to minimize reabsorption of the emitted luminescence. The $\overline{E}(^2E)$ and $2\overline{A}(^2E)$ doublets were split in a magnetic field directed along the c axis, of magnitude 1.428 T in the case of the 40 at.ppm sample, and 1.395 T for the 340 at.ppm sample. The temperature was held at 1.6 K, sufficiently low to freeze out any thermal relaxation [2].

The experimental results to be discussed here [3] are presented in Fig. 2, which shows the relaxation time between the Zeeman levels of $\overline{E}(^2E)$ as it varies with the total metastable concentration N^*. A measure for the latter was assumed to be the total luminescence emitted, whence its units relate to the number of photons counted. The relaxation was measured by perturbing the $\overline{E}(^2E)$ populations by transient microwave saturation of the connecting Zeeman transition at 48.9 respectively 47.6 GHz, and observing the subsequent recovery via the intensities of suitable Zeeman components of the R_1 luminescence (cf. Fig. 1). A small hole cut in the bottom of the TE_{102} cavity allowed optical pumping, and slits in the side wall permitted the observation of the luminescence at right angles to both the magnetic field and the incident illumination with a high-resolution monochromator. The conclusion drawn from Fig. 2 is that continuous optical pumping induces a sizeable relaxation between the Zeeman

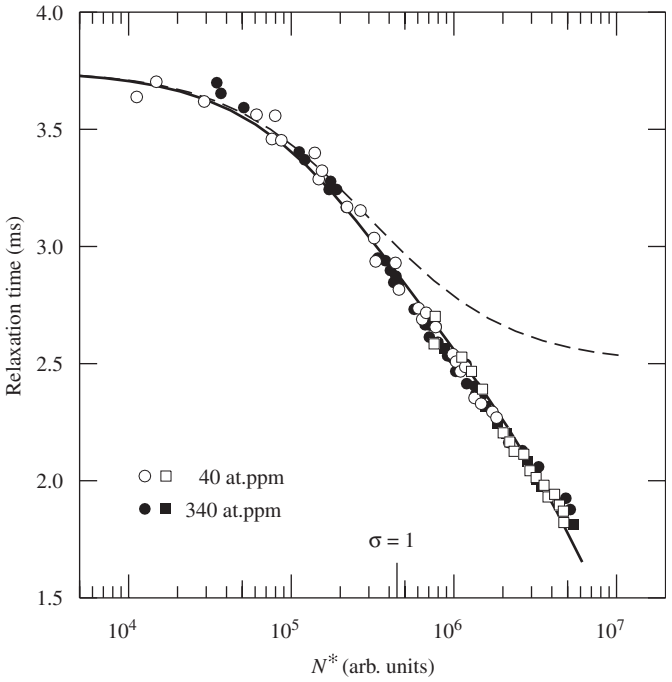

Fig. 2. Relaxation time of $\overline{E}(^2E)$ versus the metastable population density N^*. The dashed curve represents Eq. (3) with $q=0.5$. The full curve additionally includes Raman relaxation according to Eq. (8).

components of $\overline{E}(^2E)$, in addition to readjustment by optical feeding and return to $^4A_2$ on the time scale $\tau_R\approx3.7\,ms$.

At the time of our experiment, tunable dye lasers were not yet available. Optical pumping of $2\overline{A}(^2E)$ had to be achieved by the use of a mercury lamp, the red light being cut out by filters (circles in Fig. 2), or an argon laser (squares). These light sources excite even higher multiplets, notably the $^4T_2$ band, which is followed by fast nonradiative decay all the way down to $2\overline{A}(^2E)$ and, for that matter, $\overline{E}(^2E)$. For an explanation of the additional relaxation our thoughts nevertheless focused on the abundance of *resonant* phonons generated by the optical pumping, viz., the 29-cm^{-1} phonons of the four frequencies connecting the $\overline{E}(^2E)$ and $2\overline{A}(^2E)$ Kramers doublets. They proved to be only part of the truth.

To describe the associated dynamics, we relied on the equations of motion for the population densities N_i of the four levels (cf. Fig. 1 for their enumeration) as well as for the occupation numbers p_{ij} of the phonons connecting them. That is,

$$\begin{aligned}dN_1/dt = {} & M_1[(p_{13}+1)N_3 - p_{13}N_1] \\ & + M_2[(p_{14}+1)N_4 - p_{14}N_1] \\ & - N_1/\tau_R + \varphi_1 N^*,\end{aligned} \tag{1}$$

$$\begin{aligned}dp_{13}/dt = {} & M_1[(p_{13}+1)N_3 - p_{13}N_1]/\rho\Delta\nu \\ & - (p_{13}-p_{13,\mathrm{thermal}})/\tau\end{aligned} \tag{2}$$

and similar equations for N_2, N_3, N_4, p_{14}, p_{23}, and p_{24}. Here, M_1 and M_2 ($M_2/M_1\sim0.1$) are the rates of the